

Nonmetallic transport of a quasi-one-dimensional metallic Si(557)-Au surface

Hiroyuki Okino,* Rei Hobara, Iwao Matsuda, Taizo Kanagawa, and Shuji Hasegawa

Department of Physics, School of Science, University of Tokyo, 7-3-1 Hongo, Bunkyo-ku, Tokyo 113-0033, Japan

Jun Okabayashi, Satoshi Toyoda, and Masaharu Oshima

Department of Applied Chemistry, School of Engineering, University of Tokyo, 7-3-1 Hongo, Bunkyo-ku, Tokyo 113-8656, Japan

Kanta Ono

Institute of Materials Structure Science, KEK, Ibaraki 305-0801, Japan

(Received 9 February 2004; revised manuscript received 26 April 2004; published 24 September 2004)

The sheet conductivity of a Au-covered Si(557) facet surface was measured by microscopic four-point probe methods using an independently driven four-tip scanning tunneling microscope and temperature-variable monolithic probes. This surface is composed of a periodic array of Au chains and known to have a quasi-one-dimensional metallic band structure. Its surface conductivities parallel to the Au chains (σ_{\parallel}) and perpendicular to them (σ_{\perp}), were obtained separately at room temperature (RT), and the anisotropy $\sigma_{\parallel}/\sigma_{\perp}$ was ~ 3 . The temperature dependence of the surface conductivity showed a semiconductive character below RT with an activation energy of ~ 55 meV. Then it can be concluded that the transport along the Au chains is not metallic band conduction.

DOI: 10.1103/PhysRevB.70.113404

PACS number(s): 73.25.+i, 68.37.Ef, 81.16.Dn

Low-dimensional electronic systems show exotic phenomena in, e.g., phase transitions and transport properties, and have attracted a wide interest. A crystal surface is a good platform for low-dimensional physics on the atomic scale, which is expected to exhibit characters different from those of mesoscopic low-dimensional systems. Especially, steps on surfaces have been known to play a crucial role in some phenomena.¹ Recently facet surface structures have been frequently used as templates for making a quasi-one-dimensional (1D) metallic system.^{2,3} For instance, Au deposits on vicinal Si(111) surfaces represent quasi-1D systems, such as Si(111)5 \times 2-Au,^{4,5} Si(557)-Au,⁵⁻⁹ Si(335)-Au,^{6,10} Si(553)-Au,^{6,11} and Si(775)-Au facets.⁶ These facets consist of massive and periodic arrays of identical metallic atom chains over the sample surface, but we cannot prepare single atomic chains individually and separately. Therefore, the anisotropy in sheet conductivity of such a facet surface is an important quantity for estimating the conductivity of individual atomic chains.

Concerning the Si(557)-Au surface, which is the sample for the present study, the interpretation of the surface-state band structure is still under debate, such as spinon-holon bands due to the Tomonaga-Luttinger liquid character,⁷ two metallic bands,^{5,8} or one metallic and one semiconducting band.⁹ In spite of such sophisticated studies of photoemission spectroscopy (PES) of this surface, however, few transport measurements have been done so far.¹²

Wasscher¹³ and Montgomery¹⁴ discussed methods for measuring anisotropic conductivity. When we measure the resistance of an infinite two dimensional (2D) sheet having anisotropic conductivities σ_x and σ_y along the x and y directions, respectively, by linear four-point probe (4 PP) and square 4 PP methods with equidistant probe spacing, it is given by

$$R_{\text{linear}} = \frac{1}{\pi\sqrt{\sigma_x\sigma_y}} \ln 2, \quad (1)$$

$$R_{\text{square}} = \frac{1}{2\pi\sqrt{\sigma_x\sigma_y}} \ln\left(1 + \frac{\sigma_y}{\sigma_x}\right), \quad (2)$$

respectively. The current source probes are aligned along x direction for these calculations. It is obvious from Eq. (2) that the square 4 PP method provides different values of resistance by changing the probe alignment. So it enables us to obtain the σ_x and σ_y separately, which is not possible by the linear 4 PP method [Eq. (1)]. This has already been shown experimentally in previous measurements for anisotropic surface superstructure.¹⁵

Practically, however, it is not straightforward to measure the surface 2D conductivity of semiconductor crystals because the measuring current flows not only through the surface layer, but also through the substrate bulk region. As a result, contributions from surface states, a surface space-charge layer, and bulk region are included in the measured conductance. Therefore, one needs some resources to minimize the bulk contribution, such as using a silicon-on-insulator (SOI) wafer,¹⁶ shortening the probe spacing,¹⁷⁻¹⁹ and using a surface inversion layer.²⁰ The method of shortening the probe spacing (microscopic 4 PP method) has turned out to be generally effective in detecting the surface conductivity with high surface sensitivity.^{15,17-19}

In the present study, we measured the surface conductivity of the Si(557)-Au facet at room temperature (RT) by the square microscopic 4 PP method using an independently driven four-tip scanning tunneling microscope (STM),¹⁷ and also the temperature dependence by the linear monolithic microscopic 4 PP method.²¹ The coverage

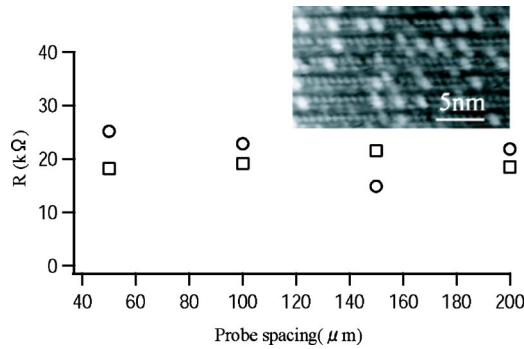


FIG. 1. Resistance measured by the linear microscopic 4PP method using the four-tip STM with changing the probe spacing. The four tips were aligned parallel to the Au chains (open circle, the average resistance = 19 ± 2 k Ω), or perpendicular to the Au chains (open square, the average resistance = 21 ± 6 k Ω). Inset is a STM image of Si(557)-Au surface taken at a single-tip STM chamber.

was 0.20 monolayer (ML), which induced a uniform Si(557)-Au facet structure.²⁵ We obtained the conductivity parallel to the Au chains (σ_{\parallel}) and perpendicular to them (σ_{\perp}) separately. They are compared with the conductivity expected from the known surface-state band structure using Boltzmann equation. The transport mechanism is discussed in relation to temperature dependence.

The anisotropic conductivity measurements were carried out at RT using our four-tip STM system installed in an ultrahigh-vacuum scanning electron microscope (UHV-SEM), combined with a capability of scanning reflection-high-energy electron diffraction (RHEED).¹⁷ Its details are described elsewhere.^{17,18} The RHEED pattern is indispensable, not only for analyzing the surface structure, but also for determining the orientation of the Au chains. The four-tip probes can be made to contact the sample surface in arbitrary arrangements with minute direct contact.

The temperature-dependent conductivity measurements were carried out using our temperature-variable monolithic microscopic 4 PP system equipped with a RHEED apparatus in UHV.²¹ We used 20 μm spacing probes, which were commercially available.²² The temperature was changed from 300–150 K using liquid N₂ (or down to 10 K using Liq. He).

A vicinal Si crystal ($15 \times 3 \times 0.525$ mm³, P-doped, $1 \sim 10$ Ω cm at RT) with a miscut of 9.45° toward the $[\bar{1}\bar{1}2]$ direction from the (111) surface was used as a substrate. Gold was evaporated from a hot alumina basket onto the substrate held at a temperature $T=700$ °C. The evaporation rate was calibrated by RHEED patterns by depositing Au on a flat Si(111) surface, following the phase diagrams in previous reports.^{23,24} A recipe for preparing the Si(557)-Au surface and the STM observations are described in Ref. 25. The inset in Fig. 1 is the STM image taken at another single-tip STM chamber. The terrace width is about 19 Å and each terrace is separated by monatomic steps as reported previously.^{8,25} Each terrace is known to contain a single Au chain.²⁶ One also notes irregular bright protrusions on a regular background of the facet.

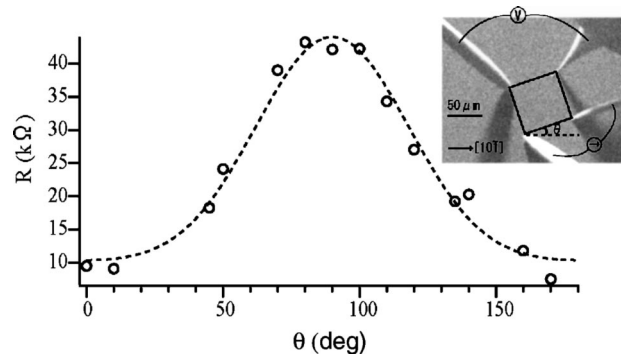


FIG. 2. Resistance measured as a function of the rotation angle θ in the square-4PP method. Probe spacing (side of the probe square) was 75 μm . Experimental data are fitted by Eq. (3). Inset is a SEM image of the probes contacting the sample surface. The Au chains run along $[10\bar{1}]$ direction (horizontal direction in this image).

Figure 1 shows the results obtained by the linear microscopic 4PP method using the four-tip STM, with changing the probe spacing. The probes were aligned along the Au chains (open circles) or in the perpendicular direction (open squares). All measurements gave similar values of resistance within the experimental error, irrespective of the probe spacing and orientation.

These results indicate two things. First, as the resistance does not depend on the probe spacing, we can say that our sample is a 2D conductor. If the current flows in a three-dimensional way in the sample, the resistance measured by the 4PP method should be inversely proportional to the probe spacing, as shown by solving the Poisson equation.^{13,17,18} In the present case, however, the electric current flows only through the surface region whose thickness is negligible compared to the probe spacing. Therefore, the measured resistance does not contain the bulk contribution of the substrate. As described later, this is due to a depletion layer at the subsurface region that electrically separates the underlying bulk region from the inversion-type surface space-charge layer.

The second point that Fig. 1 tells us is the inability to measure the anisotropic conductivity. Even by rotating the probe alignment by 90° with respect to the Au chains, the measured resistance does not change. This is expected from Eq. (1). So our sample can be regarded as an infinite 2D conductor because the sample size is much larger than the probe spacing, and we can apply Eqs. (1) and (2).

Then, the anisotropic 2D conductivity can be obtained by the square 4PP method as indicated by Eq. (2). In order to improve the measurement precision, we did the square 4PP measurements with rotating the square, i.e., a “rotational square microscopic 4PP” method.¹⁵ As shown in the inset of an SEM image in Fig. 2, the rotation angle θ is defined between the line linking the current source probes and the Au chains. By solving the Poisson equation with this probe configuration, the resistance is given as a function of θ by,¹⁵

$$R_{\text{square}}(\theta) = \frac{1}{2\pi} \frac{1}{\sqrt{\sigma_{\parallel}\sigma_{\perp}}} \times \ln \sqrt{\frac{(\sigma_{\parallel}/\sigma_{\perp} + 1)^2 - 4 \cos^2 \theta \sin^2 \theta (\sigma_{\parallel}/\sigma_{\perp} - 1)^2}{(\sin^2 \theta + \sigma_{\parallel}/\sigma_{\perp} \cos^2 \theta)^2}}. \quad (3)$$

Figure 2 shows the result of rotational square microscopic 4PP measurements with 75 μm probe spacing. By fitting Eq. (3) with the experimental data in Fig. 2, σ_{\parallel} and σ_{\perp} were obtained separately; $\sigma_{\parallel} = 9.3 \pm 0.9 \mu\text{S}/\square$ and $\sigma_{\perp} = 3.5 \pm 0.2 \mu\text{S}/\square$. The values are averages with other measurements by the same rotational microscopic 4PP method with different probe spacings. The conductivity along the Au chains is actually higher than that in the perpendicular direction. The anisotropy $\sigma_{\parallel}/\sigma_{\perp}$ is 2.7 ± 0.3 . This anisotropy is much smaller than that for a Si(111)-4 \times 1-In surface¹⁵ ($\sigma_{\parallel}/\sigma_{\perp} \sim 70$).

Next, we discuss this result by comparing the surface-state band structure already determined by PES. The measured sheet conductivities contain contributions from the surface states (σ_{ss}) and the surface space-charge layer (σ_{sc}). We can ignore the contribution of bulk (σ_b), as mentioned before, because of the 2D nature as clarified by the probe-spacing dependence in Fig. 1. According to our core-level PES measurements of the Si(557)-Au surface taken at the beamline BL-1C of the Photon Factory in KEK,²⁷ the bulk-valence-band maximum at the surface is located at 0.38 eV below the Fermi level, using a reference value of 0.63 eV for Si(111)7 \times 7 surface.²⁸ This indicates a formation of a very weak inversion layer under the surface on an *n*-type Si crystal, and a resulting *p/n* junction between the surface space-charge layer and the underlying bulk.¹⁵ A depletion layer at the *p/n* junction electrically isolates the surface layer from the underlying bulk region, so that the measurement current is confined only near the surface. This is a reason why we can ignore the σ_b .

Once we know the Fermi-level positions at the surface and in the bulk, i.e., the band bending, the sheet conductivity in the weak inversion layer σ_{sc} can be calculated by solving the Poisson equation.²⁹ The thickness of the inversion layer was calculated to be 70~260 nm, depending on the bulk resistivity $\rho = 1 \sim 10 \Omega \text{ cm}$ of our sample crystals, and σ_{sc} was estimated to be on the order of $10^{-3} \mu\text{S}/\square$. This is negligible compared with our measured sheet conductivity (on the order of $10 \mu\text{S}/\square$). Thus, we can say that *the measured conductivity comes from the surface-state conductance σ_{ss} only.*

The surface-state band structure of the Si(557)-Au facet surface has already been measured by angle-resolved PES.⁵⁻⁹ So we can calculate the conductivity from the band structure using the Boltzmann equation. For 2D conductors, it is given by³⁰

$$\sigma_{ij} = \frac{1}{2\pi^2} \frac{e^2}{\hbar} \int \tau_k \frac{v_{ki} v_{kj} dk_F}{|v_k|}, \quad (4)$$

where τ_k , k_F and $v_{ki} = [(1/\hbar)/(\partial E_k/\partial k_i)]$ are the carrier relaxation time, Fermi wave vector, and Fermi velocity along the

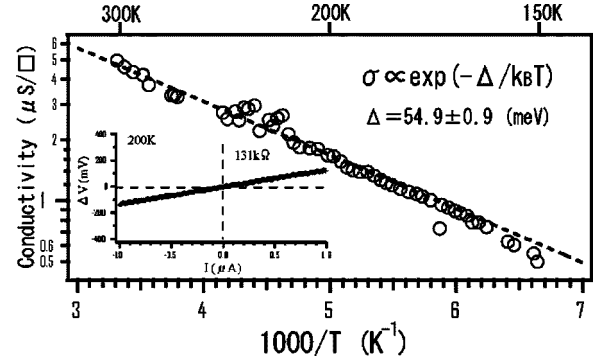


FIG. 3. Surface conductivity as a function of inverse temperature. The 20 μm spacing probes were aligned along the Au chains. Inset is a typical *I-V* curve at 200 K.

i direction at the Fermi level, respectively. The integral is done on the Fermi surface. First, according to Ref. 11, we assumed two metallic bands and used a tight-binding model of the band dispersion. After integrating Eq. (4) on the Fermi surface, the conductivity tensor was calculated to be $\sigma_{\parallel} = 1.3 \times 10^{11} \times \tau_{\parallel} [\text{S}/\square]$, where τ_{\parallel} is the mean-carrier relaxation time.

Next, by assuming that the calculated conductivities equal the measured one, we can obtain the value of τ_{\parallel} . By comparing the experimental σ_{\parallel} with the calculated one, τ_{\parallel} and the resulting mean-free path along the Au chains are estimated to be $\sim 7 \times 10^{-17} \text{ s}$ and $\sim 0.6 \text{ \AA}$, respectively. Since this mean-free path is much shorter than the lattice constant, the analysis does not make sense. In other words, *the Boltzmann picture is not applicable for the transport mechanism along the Au chains.* According to Ref. 9, one of the two surface-state bands is semiconducting. Therefore, we did the same calculation [Eq. (4)] by assuming a single metallic band. Since, however, this made just a difference of factor 2 in conductivities, the above conclusions hold.

Next we measured the temperature dependence of the sheet conductivity. Figure 3 shows the result. The conductivity exponentially decreased with cooling below RT, indicating a nonmetallic conduction. This is similar to the previous research.¹² The data points are well fitted by $\sigma \propto \exp[-\Delta/k_B T]$, giving an activation energy $\Delta = 54.9 \pm 0.9 \text{ meV}$. This behavior contradicts the PES result that the Si(557)-Au surface has a metallic band at RT.

What is the nature of the electrical conduction along the Au chains? By recalling the dense and irregular bright protrusions on the Au chains in the STM image, which are said to be extra Si atoms⁶ (inset of Fig. 1), they seem to cut the chains into rods. In such a case, conduction is described in terms of variable range hopping (VRH).³¹ In our temperature range, VRH tells us that the conductivity is of activated type hopping conduction ($\sigma \propto \exp[-\Delta/k_B T]$), with the activation energy $\Delta \sim e^2/4\pi\epsilon l$ where ϵ is a dielectric constant and l is the rod length. By using for the value of the dielectric constant that of bulk Si value ($\epsilon = 11.7\epsilon_0$, where ϵ_0 is a dielectric constant of vacuum) and l as 7.5 nm, Δ was calculated as $\sim 16 \text{ meV}$. The difference between this value and our measurement value of 55 meV is due to the overestimation of the dielectric constant ϵ . In the case of

Si(111)-4×1-In surface,¹⁵ for comparison, no such irregularities exist on the chains, so that the Boltzmann picture is quantitatively applicable. Or the band structure itself can be altered to be semiconducting by the dense protrusions. For the Si(111)5×2-Au surface, these protrusions change the metallic chains into semiconducting chains due to electron doping.^{32,33} The same thing may happen on the Si(557)-Au surface, which divides the surface into metallic region and semiconducting region. This is also the possible reason for the semiconducting behavior of the transport measurement and the metallic behavior of the PES measurement.

In summary, we have applied the rotational square micro-4PP method and the temperature-variable monolithic linear micro-4PP method to a quasi-1D system of Si(557)-Au fac-

ets. The conductivities along the Au chains (σ_{\parallel}) and across them (σ_{\perp}) were separately obtained. The ratio between them $\sigma_{\parallel}/\sigma_{\perp}$ was ~ 3 . The temperature dependence of the surface conductivity revealed a semiconducting character. It, thus, turned out that metallic band conduction does not occur along the Au chains in spite of the metallic band structure revealed by PES. Dense irregularities, such as protrusions on the Au chains observed in STM images, would play an important role to cause such a nonmetallic conduction.

Dr. K. Yoo and Dr. J.R. Ahn are gratefully acknowledged for their valuable discussions. This work has been supported by Grants-In-Aid from Japanese Society for the Promotion of Science.

*Corresponding author. Electronic address:

okino@surface.phys.s.u-tokyo.ac.jp

- ¹M. Ueno, I. Matsuda, C. Liu, and S. Hasegawa, *Jpn. J. Appl. Phys., Part 1* **42**, 4894 (2003).
- ²F. J. Himpsel, A. Kirakosian, J. N. Crain, J.-L. Lin, and D. Y. Petrovykh, *Solid State Commun.* **117**, 149 (2001).
- ³A. Mugarza, A. Mascaraque, V. Pérez-Dieste, V. Repain, S. Rousset, F. J. García de Abajo, and J. E. Ortega, *Phys. Rev. Lett.* **87**, 107601 (2001).
- ⁴I. Matsuda, M. Hengsberger, F. Baumberger, T. Gerber, H. W. Yeom, and J. Osterwalder, *Phys. Rev. B* **68**, 195319 (2003).
- ⁵K. N. Altmann, J. N. Crain, A. Kirakosian, J.-L. Lin, D. Y. Petrovykh, and F. J. Himpsel, *Phys. Rev. B* **64**, 035406 (2001).
- ⁶J. N. Crain, J. L. McChesney, Fan Zheng, M. Gallagher, P. C. Snijders, M. Bissen, C. Gundelach, S. C. Erwin, and F. J. Himpsel, *Phys. Rev. B* **69**, 125401 (2004).
- ⁷P. Segovia, D. Purdie, M. Hengsberger, and Y. Baer, *Nature (London)* **402**, 504 (1999).
- ⁸R. Losio, K. N. Altmann, A. Kirakosian, J.-L. Lin, D. Y. Petrovykh, and F. J. Himpsel, *Phys. Rev. Lett.* **86**, 4632 (2001).
- ⁹J. R. Ahn, H. W. Yeom, H. S. Yoon, and I.-W. Lyo, *Phys. Rev. Lett.* **91**, 196403 (2003).
- ¹⁰P. Starowicz, O. Gallus, Th. Pillo, and Y. Baer, *Phys. Rev. Lett.* **89**, 256402 (2002).
- ¹¹J. N. Crain, A. Kirakosian, K. N. Altmann, C. Bromberger, S. C. Erwin, J. L. MacChesney, J.-L. Lin, and F. J. Himpsel, *Phys. Rev. Lett.* **90**, 176805 (2003).
- ¹²M. Schöck, C. Sürgers, and H. v. Löhneysen, *Thin Solid Films* **428**, 11 (2003).
- ¹³J. D. Wasscher, *Philips Res. Rep.* **16**, 301 (1961).
- ¹⁴H. C. Montgomery, *J. Appl. Phys.* **42**, 2971 (1971).
- ¹⁵T. Kanagawa, R. Hobara, I. Matsuda, T. Tanikawa, A. Natori, and

- S. Hasegawa, *Phys. Rev. Lett.* **91**, 036805 (2003).
- ¹⁶K. Yoo and H. H. Weitering, *Phys. Rev. Lett.* **87**, 026802 (2001).
- ¹⁷I. Shiraki, F. Tanabe, R. Hobara, T. Nagao, and S. Hasegawa, *Surf. Sci.* **493**, 633 (2001); S. Hasegawa, I. Shiraki, F. Tanabe, and R. Hobara, *Current Appl. Phys.* **2**, 465 (2002).
- ¹⁸I. Shiraki, T. Nagao, S. Hasegawa, C. L. Petersen, P. Boggild, T. M. Hansen, and F. Grey, *Surf. Rev. Lett.* **7**, 533 (2000).
- ¹⁹S. Hasegawa and F. Grey, *Surf. Sci.* **500**, 84 (2002).
- ²⁰T. Tanikawa, I. Matsuda, T. Kanagawa, and S. Hasegawa, *Phys. Rev. Lett.* **93**, 016801 (2004).
- ²¹T. Tanikawa, I. Matsuda, R. Hobara, and S. Hasegawa, *e-J. Surf. Sci. Nanotech.* **1**, 50 (2003).
- ²²See Capres; <http://www.capres.com/>
- ²³R. Plass and L. D. Marks, *Surf. Sci.* **380**, 497 (1997).
- ²⁴T. Nagao, K. Tsuchie, S. Hasegawa, and S. Ino, *Phys. Rev. B* **57**, 10100 (1998).
- ²⁵H. Okino, I. Matsuda, T. Tanikawa, and S. Hasegawa, *e-J. Surf. Sci. Nanotech.* **1**, 84 (2003).
- ²⁶D. Sánchez-Portal and R. M. Martin, *Surf. Sci.* **532–535**, 655 (2003).
- ²⁷H. Okino *et al.* (unpublished).
- ²⁸F. J. Himpsel, G. Hollinger, and R. A. Pollak, *Phys. Rev. B* **28**, 7014 (1983).
- ²⁹H. Lüth, *Surfaces and Interfaces of Solid Materials* (Springer-Verlag, Berlin, 1995).
- ³⁰T. Hamaguchi and K. Taniguchi, *Physics of Semiconductor Device* (Asakura Publishing, Tokyo, 1990), in Japanese.
- ³¹M. M. Fogler, S. Teber, and B. I. Shklovskii, *Phys. Rev. B* **69**, 035413 (2004).
- ³²S. C. Erwin, *Phys. Rev. Lett.* **91**, 206101 (2003).
- ³³H. S. Yoon, S. J. Park, J. E. Lee, C. N. Whang, and I.-W. Lyo, *Phys. Rev. Lett.* **92**, 096801 (2004).